# 2Pb5-6

## Verification of the influence of microstructure in the liver on the evaluation of shear wave velocity
## 肝臓内のミクロ構造がせん断波速度評価に与える影響の検証

Daiki Ito[1†], Takuma Oguri[1,2], Mikio Suga[3] and Tadashi Yamaguchi[3*] ([1]Grad.School Sci. and Eng., Chiba Univ; [2]2Ultrasound General Imaging, GE Healthcare; [3]Center for Frontier Medical Engineering, Chiba Univ.)
伊藤 大貴[1†], 大栗 拓真[1,2], 菅 幹生[3], 山口 匡[3*] ([1]千葉大院　融合理工学府, [2]GE ヘルスケア・ジャパン 超音波製品開発部, [3]千葉大 CFME)

### 1. Introduction

Shear wave elastography (SWE) can quantitatively evaluate tissue stiffness based on shear wave velocity (SWV) propagating in biological tissues and is used to evaluate the progression of liver fibrosis. In recent years, the evaluation of the degree of fat deposition in the liver is expected. However, previous studies have been shown that the evaluation results of SWE were unstable due to factors as liver structure and complexity of physical properties [1].

In this studys, shear wave propagating in biological tissues was simulated by the elastic finite-difference time domain (FDTD) method [2] under the transmisson condition mimicked the distribution of acoustic radiation force (ARF) in an clinical diagnosis equipment. To standardize SWE of the liver , the influence of microstructure (fatty droplets and fiber tissues) in the liver on SWV evaluation was verified by shear wave propagating simulation.

### 2. Method

#### 2.1 Simulation

Propagation of shear wave was simulated in two dimensions with the elastic FDTD method by adding the ARF distributions. ARF was mimicked acoustic field of push pulse of abdominal linear array probe (9L-D, GE Healthcare) of ultrasonic equipment (LOGIQ S8, GE Healthcare). By adding this ARF to the left edge of the simulation space, shear wave was propagated for the lateral direction in the simulation space of 20 mm × 10 mm (2000 pixel × 1000 pixel; 1 pixel = 10 μm). The schematic of simulation space is shown in **Fig. 1**. Beneger's boundary condition was used due to eliminate unwanted reflections at the end of the simulation space.

The area of 5 mm × 5 mm (green area on left figure) in the simulation space was placed the biological tissue structure that were reproduced from pathological images of the actual livers. Different SWVs were set for the liver, fat droplets, and fibers

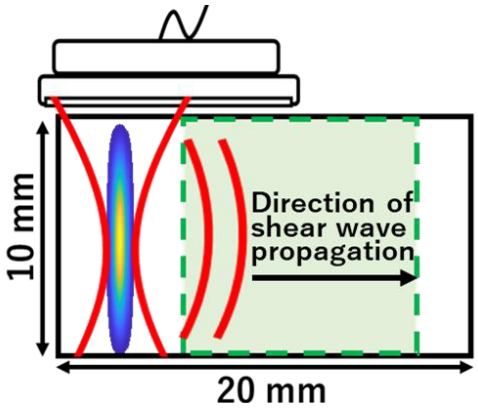


**Fig.1 Schematic image of simulation space**

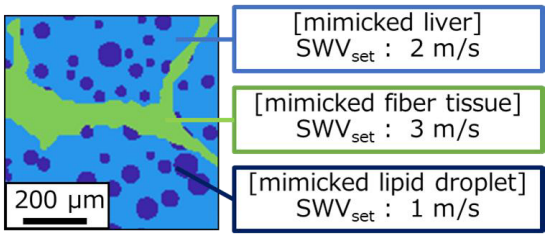


**Fig.2 Simulation model mimicked NASH liver**

as $SWV_{set}$ set as shown in **Fig. 1**. The simulation model of NASH liver is shown in **Fig. 2** as an example.

The propagation of shear wave in lateral direction (Left → Right) was reproduced from time change of particle velocity in the depth direction that obtained from the simulation. The wavelength and frequency of shear wave propagating in homogeneous liver were 3.89 mm and 216 Hz.

#### 2.2 Analysis of SWV_evaluated

$SWV_{eva}$ of each tissue were obtained using a time difference calculated by a cross-correlation method from two timewaves of the particle velocity continuous in the lateral direction [3]. Before the analysis, the particle velocity distribution was processed to remove the waves propagation in the opposite direction of shear wave (the negative direction of the lateral direction).

†d.ito@chiba-u.jp, *yamaguchi@faculty.chiba-u.jp

## 3. Results

### 3.1 SWV of fatty liver

**Figure 3(a)** shows the simulation models and evaluated $SWV_{eva}$ distribution (SWV map) of fatty livers that fat ratio of 21.30% and 37.63%. $SWV_{eva}$ was slowed even in the fat droplets that are smaller than the wavelength of shear wave. In the micro, it was confirmed to occur reflection and diffraction of shear waves in fat droplets and to change of shear wavelength temporary at the boundaries of different tissues. The distortion of shear waveform and other wave affected the detection and analysis of shear waves, accordingly, $SWV_{eva}$ around the fat droplet fluctuated. The fluctuation became remarkable as fat droplets became denser.

**Figure 3(b)** shows the boxplot and average of SWV in fatty liver that fat ration of 11.03%, 21.30% and 37.63% at whole analysis area. In macro, the decrease of $SWV_{eva}$ is smaller than the rate of increase of fat droplets due to the interaction and averaging of micro phenomena.

### 3.2 SWV of liver fibrosis

**Figure 3(c)** shows the simulation models and evaluated SWV map of liver fibrosis that fiber ration of 15.87% and 23.89%. $SWV_{eva}$ tended to differ depending on the shape of fiber tissues. Especially, when fiber tissues existed in the direction orthogonal to the propagation direction of shear wave, the propagation of shear wave becomes spatially inhomogeneous. Also, Shape change of shear wave due to fibrous tissue greatly influences subsequent propagation. With this, the accuracy of $SWV_{eva}$ evaluation decreased with the passage of time.

**Figure 3(d)** shows the boxplot and average of SWV in liver fibrosis that fiber ration of 15.87%, 23.89%, 36.66% at whole analysis area. In macro, the average of $SWV_{eva}$ is much larger than the simple average $SWV_{eva}$ analyzed from $SWV_{set}$. The tendency became remarkable as fiber ratio in liver become increased.

## 4. Conclusion

The relationship between the liver (containing fat droplets and fiber tissues) and SWV evaluation was verified using shear wave propagation simulation by the elastic FDTD method. In fatty liver, the shear wave changes microscopically due to the deposition of lipid droplets in the liver, and the local SWV has various values. In SWV evaluation in a macroscopic region such as in clinical equipment, local variability tends to be averaged and tends to approach the value of SWV in healthy liver. In liver fibrosis, local SWV tends to be faster due to the fiber tissues, and macro evaluation strongly reflects microscopic characteristics compared to fatty liver.

A simulation of a NASH model in which fat droplets and fiber tissues are mixed in the liver shows that the average and variance of the evaluation value of $SWV_{eva}$ differs due to the difference in the mixing ratio of fat and fibers.

**Acknowledgment**

This work was partly supported by JSPS Core-to-Core Program, KAKENHI 19H04482, the Institute for Global Prominent Research at Chiba University, and conducted as part of the activities of the JSUM SWE Standardization Subcommittee and JRS J-QIBA.

**References**

1.Mark L. Palmeri , et al; IEEE T. Ultrason, 64(2017),
2. S. masahiro, ASJ, 64(2008),
3. Y makoto, Med. Image. Tech. 32(2014)

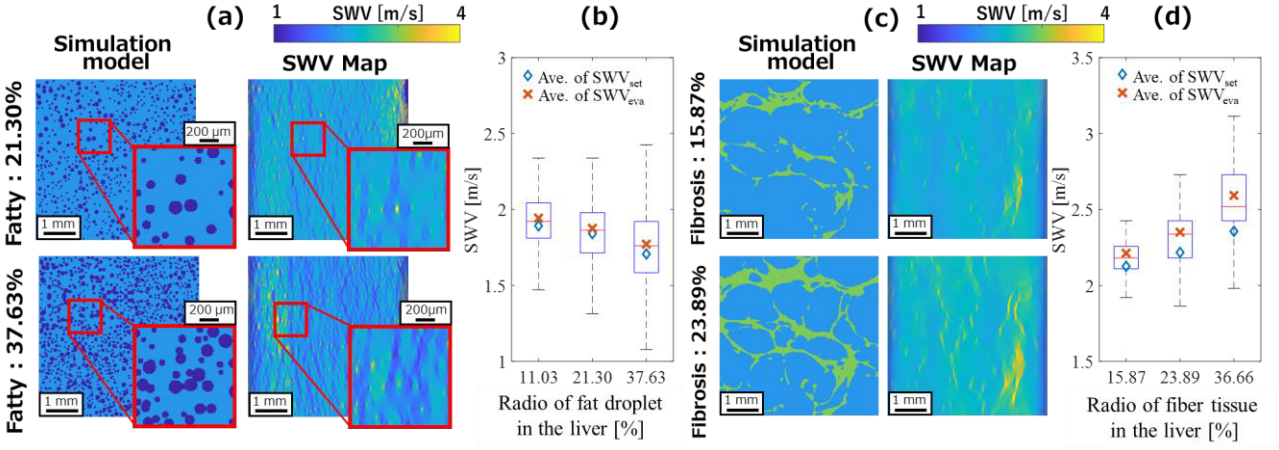


**Fig.3 Simulation results of shear wave propagation in each liver. (a) simulation models and SWV maps of fatty liver, (b) boxplot and average of $SWV_{eva}$ of fatty liver, (c) simulation models and SWV maps of liver fibrosis, (d) boxplot and average of $SWV_{eva}$ of liver fibrosis.**